Late Cretaceous adakitic magmatism in east-central Sonora, Mexico, and its relation to Cu-Zn-Ni-Co skarns

Efrén Pérez-Segura[1,*], Eduardo González-Partida[2], and Victor A. Valencia[3]

[1] Departamento de Geología, Universidad de Sonora,
Rosales y Boulevard Luis Encinas, 83000 Hermosillo, Sonora, Mexico.
[2] Centro de Geociencias, Universidad Nacional Autónoma de México,
Campus Juriquilla, 76230 Querétaro, Qro., Mexico.
[3] Department of Geosciences, The University of Arizona,
Gould-Simpson Building, 1040 East Fourth St., 85721-0077 Tucson, Arizona, USA.
**efrenpese@yahoo.com*

ABSTRACT

The Late Cretaceous-early Tertiary (Laramide) orogeny (90–40 Ma) in the northwestern part of Mexico produced an important calc-alkaline magmatism, accompanied by several associated porphyry copper and skarn deposits. In the Sierra Santo Niño, Sonora, the Bacanora batholith intrusive complex, composed of tonalite-granodiorite and biotite-hornblende granites intrudes both upper Paleozoic platform sedimentary rocks and Upper Cretaceous volcanic rocks, and is intruded by the San Lucas porphyry (quartz monzonite). The Bacanora batholith and the San Lucas porphyry yield crystallization ages between ~91 Ma and ~89 Ma, and represent the oldest Late Cretaceous intrusive event yet reported for east-central Sonora. Cu-Zn-Ni-Co skarn deposits were generated by this magmatism, and have not been previously described in Sonora. The Bacanora batholith and the San Lucas porphyry show average compositions of 65.1–65.3 wt.% SiO_2 and 15.7 wt.% Al_2O_3; the main geochemical differences among both units are in 4.3 wt.% Fe_2O_3, 1.9 wt.% MgO, 3.8 wt.% CaO and 3.3 wt.% K_2O for the Bacanora batholith versus 2.8 wt.% Fe_2O_3, 1.7 wt.% MgO, 2.1 wt.% CaO and 5.1 wt.% K_2O for the San Lucas porphyry. Both units show a LREE enrichment as well as HREE depletion. These compositions match with that of adakitic magmas produced by partial melting of subduced oceanic slab, leaving garnet and amphibole in the restite.

Key words: magmatism, geochronology, adakite, skarn, Sonora, Mexico.

RESUMEN

La orogenia del Cretácico Tardío-Terciario temprano o Laramide (90–40 Ma) en el noroeste de México produjo un importante magmatismo calcialcalino, acompañado por diversos yacimientos asociados de tipo pórfido cuprífero y skarn. En la Sierra Santo Niño, Sonora, el complejo intrusivo del batolito Bacanora, compuesto de tonalita-granodiorita y granitos de biotita-hornblenda intrusiona tanto una plataforma de rocas sedimentarias del Paleozoico superior, como rocas volcánicas de Cretácico Superior, y es intrusionado a su vez por el pórfido de cuarzo-monzonita San Lucas. El batolito Bacanora y el pórfido San Lucas arrojan edades de cristalización entre ~91 Ma y ~89 Ma, y representan el evento intrusivo del Cretácico Tardío más antiguo reportado hasta ahora en Sonora centro-oriental. Algunos skarns de Cu-Zn-Ni-Co fueron generados por este magmatismo y no habían sido descritos previamente en Sonora. El batolito Bacanora y el pórfido San Lucas muestran una composición promedio de 65.1–65.3% de SiO_2 y 15.7% Al_2O_3; las principales diferencias geoquímicas son 4.3% Fe_2O_3, 1.9% MgO, 3.8% CaO

Pérez-Segura, E., González-Partida, E., Valencia, V.A., 2009, Late Cretaceous adakitic magmatism in east-central Sonora, Mexico, and its relation to Cu-Zn-Ni-Co skarns: Revista Mexicana de Ciencias Geológicas, v. 26, núm. 2, p. 411-427.

y 3.3% K_2O para el batolito Bacanora versus 2.8% Fe_2O_3, 1.7% MgO, 2.1% CaO y 5.1% K_2O para el pórfido San Lucas. Ambas unidades muestran un enriquecimiento en LREE así como una disminución en HREE. Estas composiciones concuerdan con un origen a partir de magmas adakíticos producidos por fusión parcial de una placa oceánica subducida,en la cual queda una restita con granate y anfíbol.

Palabras clave: magmatismo, geocronología, adakitas, skarns, Sonora, México.

INTRODUCTION

The Late Cretaceous-early Tertiary (Laramide) orogeny is recognized in Sonora as a minor ductile compressive tectonic event (Rangin, 1982; Pubellier, 1987; Pubellier *et al.*, 1995) responsible for an important magmatic event that occurred between 90–40 Ma (Damon *et al.*, 1981; Damon, 1986). Subduction of the Farallon plate under North America (Coney and Reynolds, 1977; Damon *et al.*, 1983a) produced a continental margin magmatic arc that migrated from west to east from the paleotrench over time. This magmatic arc lay parallel to the northwestern Mexico Pacific coast and originated the Sonoran batholith (Damon *et al.*, 1983b) and correlative volcanic rocks (McDowell *et al.*, 2001; Roldán-Quintana, 2002) that crop out extensively along NNW trending ranges. The magmatism has been traditionally considered to be calc-alkaline (Roldán-Quintana, 1991, 1994, 2002; Valencia-Moreno *et al.*, 1999, 2001, 2003). Most of the mineral deposits, including porphyry copper and associated skarns are spatially and temporally related to this magmatism (Clark *et al.*, 1979, 1982; Damon *et al.*, 1981, 1983a; Pérez-Segura, 1985; Barton *et al.*, 1995; Staude and Barton, 2001; Valencia-Gómez, 2005; Barra *et al.*, 2005).

This work provides new geochemical and geochronological evidence of intrusive rocks in the Sierra Santo Niño (east-central Sonora), and the genetic relationship between intrusions and recently discovered Cu-Zn-Ni-Co mineralization (Pérez-Segura *et al.*, 2004). The intrusive rocks of Sierra Santo Niño have an adakitic signature, as defined by Defant and Drummond (1990), and were emplaced at the beginning of the Late Cretaceous-early Tertiary orogeny.

GEOLOGICAL SETTING

The study area is located 150 km east of the city of Hermosillo in the Basin and Range Province of Sonora, northwestern Mexico (Figure 1). The morphology of the Sierra Santo Niño is defined by Tertiary extension, which occurred in Sonora at *ca.* 25–10 Ma (McDowell *et al.*, 1997; Gans, 1997). The Sierra Santo Niño is a horst that is structurally bound at the east by the Bacanora semi-graben and at the west by the Río Yaqui graben (Figure 1).

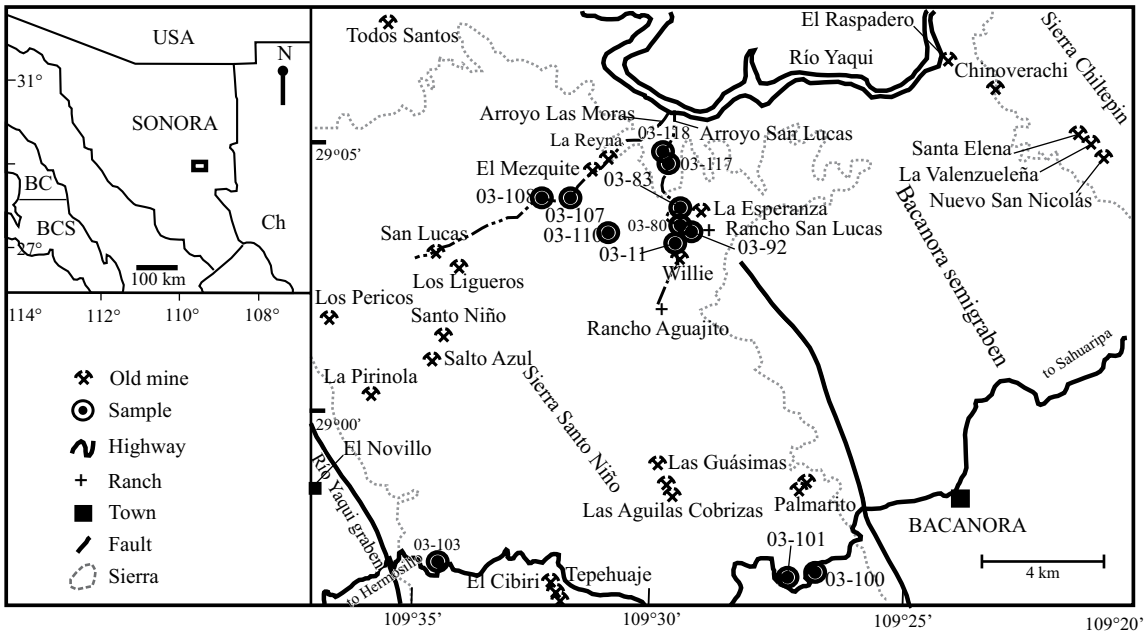

Figure 1. Location of study area, showing geographic features, main mineralized zones and sites of sampling. N: North, Ch: Chihuahua, BC: Baja California, BCS: Baja California Sur, USA: United States of America.

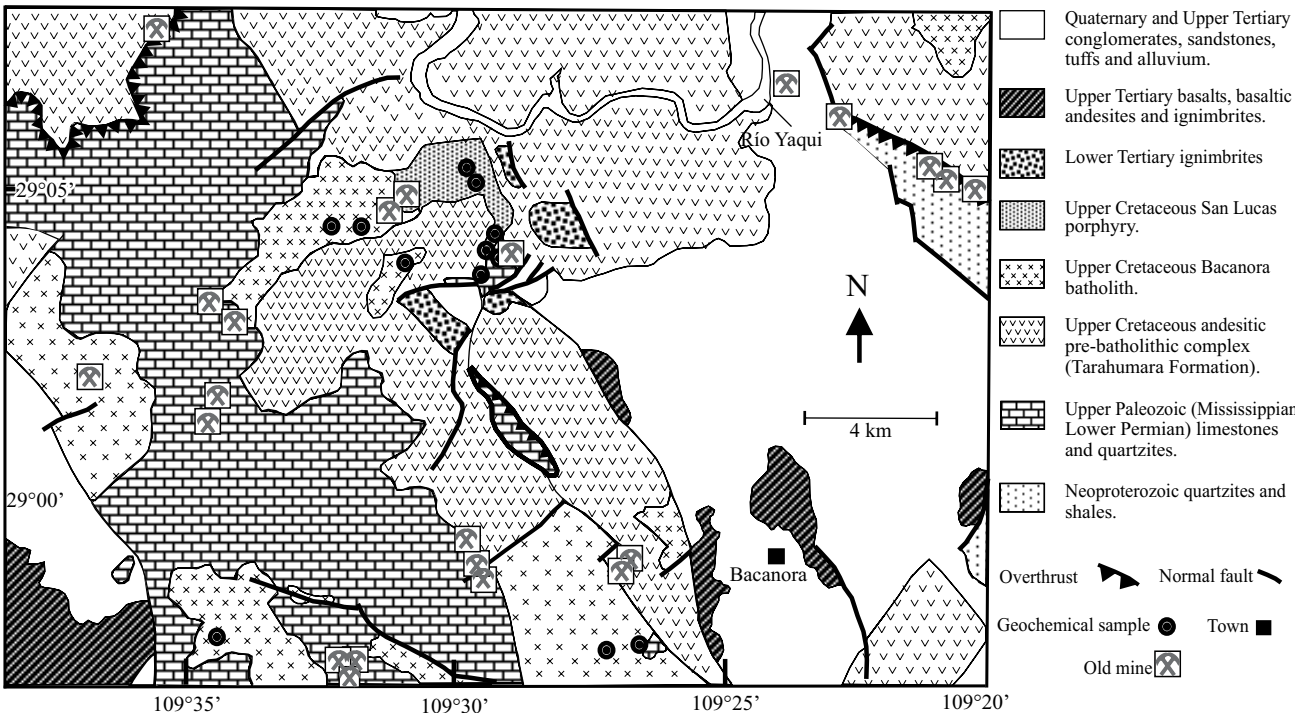

Figure 2. Generalized geological map of the study area (same area of Figure 1) modified from Servicio Geológico Mexicano (formerly Consejo de Recursos Minerales, 1995, 2005).

The geology of the area (Figure 2) has been previously described in the Santa Teresa (H12D-47) and Bacanora (H12D-55) geological maps edited by the Servicio Geológico Mexicano (formerly Consejo de Recursos Minerales, 1996, 2005). The highest portions of the Sierra Santo Niño are composed of Paleozoic sedimentary platform rocks, also recognized at the southern part of this range (Araux and Vega, 1984) and at the Sierra Agua Verde, northwest of the study area (Ochoa and Sosa, 1993; Stewart *et al.*, 1999). The sedimentary rocks in the Sierra Santo Niño represent a roof pendant resting on granitic bodies. In the northern part of the study area (at the Todos Santos mine), Paleozoic platform rocks are thrust over pre-batholithic andesitic rocks, which are correlated with the Tarahumara Formation (Wilson and Rocha, 1946; McDowell *et al.*, 2001; Roldán-Quintana, 2002).

Paleozoic rocks

Paleozoic rocks are well exposed along the Novillo-Bacanora highway and can be observed from 600 m (above sea level) up to the peak of the Sierra Santo Niño at 1600 m. The strata have a general orientation of N45°W and dip 40° SW in the northwestern portion of the range. Rocks are composed of meter-thick beds of marble, massive limestone, and thin (~10–20 cm) layers of metamorphosed, pyrite-bearing siliceous limestone. The thickness of the Paleozoic section is estimated as 600 m. The carbonate rocks of the northern Sierra Santo Niño, between El Novillo town and the La Esperanza mine, are related to the Mississippian-early Permian rocks described in the southern Sierra Santo Niño by Araux and Vega (1984) and in the Sierra Agua Verde by Stewart *et al.* (1999). Fossil corals observed at the Todos Santos mine indicate a possible Mississippian age (Stevens, 2005, written communication).

The Late Cretaceous andesitic pre-batholithic complex: Tarahumara Formation

The Tarahumara Formation was originally identified by Wilson and Rocha (1946) at the Cañón del Obispo, located 65 km south of Bacanora. The Tarahumara Formation consists of andesitic and dacitic lava flows, volcanic breccias and pyroclastic deposits (McDowell *et al.*, 2001). The thickness is up to 2500 m. The Tarahumara Formation has been interpreted as the volcanic equivalent of the Sonoran batholith, and has been dated using U-Pb isotopes in zircons with ages that range from 90 to 70 Ma (McDowell *et al.*, 2001; Roldán-Quintana, 2002).

Rocks correlated with the Tarahumara Formation in the study area form extensive andesitic outcrops, which are ubiquitous in east-central Sonora. They are massive green andesite, andesitic tuff and volcaniclastic rocks. Commonly, these rocks are hydrothermally altered to chlorite + epidote + calcite + quartz + pyrite, and are black in color due to the presence of abundant secondary biotite. The thickness of these rocks is estimated to be up to 1500 m. At the Rancho Aguajito (Figure 1), andesitic rocks have been altered by

contact metasomatism to garnet + pyroxene. In the northern part of the Sierra Santo Niño (at the Todos Santos mine), the andesitic rocks are thrust by Paleozoic limestones and in northern Sierra Chiltepín by Neoproterozoic clastic rocks (Figure 2).

INTRUSIVE MAGMATISM IN THE SIERRA SANTO NIÑO

The Bacanora batholith and the San Lucas porphyry

Rocks of the Bacanora batholith crop out in three main areas: 1) along the Arroyo Moras, in a 14 km^2 band; 2) east of the Novillo town in a 10 km^2 strip; and 3) along the El Novillo-Bacanora highway (Figure 1). It represents about 25 % of the surface of Sierra Santo Niño observed in Figure 2. Morphology, geological relationships and geophysical observations compiled in the Servicio Geológico Mexicano maps, suggest that the observed outcrops are the surficial expression of a major batholithic body at depth. The Bacanora batholith likely comprises a complex intrusive suite; the predominant lithology is granodiorite, varying from tonalite to *sensu-stricto* granite. The common mafic minerals are hornblende and biotite, but pyroxene is locally present. Pegmatite, aplite and lamprophyric dikes commonly crosscut the batholith.

The San Lucas porphyry is a hypabisal intrusive to subvolcanic body with an elongated or amoeboid shape. It is exposed within a 5 km^2 area along the Arroyo San Lucas, between the Rancho San Lucas and the Río Yaqui, and forms about 6 % of the Bacanora batholith outcrop. The San Lucas porphyry intrudes limestones, quartzites and conglomerates inferred to be late Paleozoic in age, and the Late Cretaceous Tarahumara andesite (Figure 2). Andesitic dikes intrude the Bacanora batholith in the Arroyo Las Moras and the metamorphosed sedimentary rocks in the Arroyo San Lucas.

Relation to Cu-Zn-Ni-Co skarns

Several ore bodies were developed along the contact zones between the intrusive bodies of the Bacanora batholith and the San Lucas porphyry, and the Paleozoic strata, *e.g.* the La Reyna, El Mezquite, Los Ligueros, San Lucas and Las Aguilas Cobrizas old mines (Figs. 1). They are skarn-type deposits containing significant Cu + Zn concentrations. A few kilometers south of the study area, in the Sierra La Campanería, other skarns contain W.

The La Esperanza skarns are the most important of these prospects and have only recently been described by Pérez-Segura *et al.* (2004). A preliminary economic evaluation suggests the existence of more than 1 Mt of ore with values around 1 g/t Au, 1–2% Cu, 1–2% Zn, 0.1–0.2% Ni and 0.1–0.2% Co. Most noteworthy is that the La Esperanza deposit is the first Ni-Co bearing ore body reported in Sonora, suitable for exploration. The mineralization was developed in the endoskarn zone in the contact between the San Lucas porphyry and the Paleozoic cover. Skarns contain a prograded assemblage with garnet more abundant than pyroxene, and a discrete retrograde assemblage with chlorite + epidote + calcite + quartz + magnetite + pyrite + siegenite [$(Ni,Co)_3S_4$] + chalcopyrite + sphalerite + hematite. Garnet composition is andraditic, whereas pyroxenes are diopsidic. Siegenite is the main Ni-Co mineral and is earlier than the deposition of the sphalerite and chalcopyrite assemblage. The ore mineralogy coupled with andraditic garnet > diopsidic pyroxene, the presence of pyrite-magnetite-hematite, and the absence of pyrrhotite, indicate that La Esperanza may be classified as an oxidized skarn (Meinert, 1998). The spatial and temporal relationship between the skarns (endoskarn) and the San Lucas porphyry, and consequently with this magmatim, is evident.

Petrography of the Bacanora batholith and the San Lucas porphyry

Two main petrographic assemblages are recognized in the Bacanora batholith: a pyroxene + biotite tonalite-syenogranite and a hornblende-biotite-bearing monzodiorite-quartzmonzonite-granodiorite-monzogranite assemblage. The contacts among different facies were not observed in the field, suggesting a gradational transition.

The pyroxene+biotite tonalite is phaneritic, fine to coarse-grained (0.5–3 mm), and commonly hypidiomorphic. Compositionally, the rocks range from a pyroxene+ biotite tonalite to a pyroxene syenogranite. Mineralogy was identified in thin section and percentages were estimated by volume; the anorthite content in plagioclase was estimated by using selected extinction angles on sections perpendicular to 010 cleavage. The modal composition is the following: quartz (5–10%), K-feldspar (5–56%), plagioclase (10–55%), pyroxene (15–20%), biotite (0–4%) and opaque minerals (3–10%). Accessory minerals are apatite, sphene and zircon. Quartz is always interstitial and is observed in myrmekitic intergrowth with feldspar in some cases. K-feldspar is orthoclase, with large crystals (~3 mm) commonly with Carlsbad twinning. The plagioclase composition is An_{30-32}. The pyroxene is most likely augite. Biotite is pleochroic and frequently has apatite and pyroxene inclusions. Sericite in plagioclase and actinolite in pyroxene are present as selective alteration minerals.

Hornblende+biotite-bearing intrusive rocks are phaneritic with grain size of 0.2 to 3 mm. They contain quartz (5–30%), K-feldspar (10–45%), plagioclase (30–60%), hornblende (5–10%) and biotite (0–10%). The accessory minerals are apatite, sphene, zircon, and opaques. K-feldspar is present as orthoclase and microcline. Quartz is interstitial. The plagioclase composition is An_{24-34}. There are traces of selective mineral alteration that consist of actinolite in

hornblende, chlorite + epidote in biotite, and sericite in plagioclase.

The San Lucas porphyry contains plagioclase and mafic phenocrysts, in an aphanitic, typically pink, groundmass. Phenocrysts are 1 to 5 mm in length, increasing in size and abundance northwards in the Arroyo San Lucas outcrop. Phenocrysts are typically plagioclase, but hornblende and biotite phenocrysts have also been observed. Orthoclase phenocrysts and quartz eyes are less common. The phenocryst composition is plagioclase, biotite, hornblende, orthoclase and quartz. The groundmass is fine-grained felsitic, and commonly microlithic to trachytic in texture, suggesting a hypabysal to subvolcanic emplacement. Plagioclase crystals are idiomorphic as thin sheets, with polysynthetic twinning, zonal structure, and a composition of An_{20-34} (oligoclase-andesine); they exhibit corroded edges. Quartz eyes commonly show three-phase fluid inclusions with NaCl crystals. Hornblende is locally altered to fibrous actinolite. Biotite is dark, appearing to be iron-rich, and frequently is altered to chlorite+calcite+epidote+opaque minerals (propylitic alteration). The groundmass is predominately composed of K-feldspar. Among the accessory minerals apatite is present and zircon crystals are idiomorphic, with prismatic shapes with a length/width ratio >2/1. Magnetite is the most common opaque mineral, although pyrite is associated with chlorite. Alteration minerals are selective: plagioclase is altered to sericite, while ferromagnesian minerals are altered to chlorite+carbonate+epidote+sphene+rutile+opaque minerals.

Geochronology

Two samples from the Bacanora batholith (03-107) and the San Lucas porphyry (03-11) were selected for zircon U-Pb geochronological analysis. Mercator coordinates of these samples are: 3216 450 N, 642 249 E for 03-107, and 3215 270 N, 646 945 for 03-11 (Figure 1). Analysis were performed by laser-ablation multicollector-inductively-coupled plasma-mass-spectrometry (LA-MC-ICPMS) at the Arizona LaserChron Center, following procedures by Valencia *et al.* (2005). Zircons were separated from 5 kg rock samples using standard techniques of the University of Arizona. Around 50 euhedral inclusion-free zircon crystals were mounted along with SL2 standards (Gehrels *et al.*, 2008) on centers of one inch phenolic O-rings, polished to expose grain interiors, and imaged with cathodoluminiscence. Analysis were performed in crystal cores and tips. Each measurement cycle consisted of one 20 s integration on every centered peak with the laser off for background counts, twenty 1 s integrations during mineral blasting, and ~30 s of purging. Zircons were ablated with a New Wave Research DUV193 ArF Excimer laser (wavelength = 193 nm). The laser beam was operated at ~60mJ energy (at 23.5kV), a pulse rate of 8Hz, and a spot size of 35 μm. The generated pit was ~12 μm deep. Ablated material was carried in helium gas mixed with Ar gas into an Isoprobe ICPMS (GV Instruments). U, Th and Pb isotopes were analyzed simultaneously in static mode using Faraday collectors for ^{238}U, ^{232}U, ^{208}Pb, ^{207}Pb and ^{206}Pb, and an ion counter for ^{204}Pb. Contributions to the 204 mass by Hg were removed by subtracting background counts. Common Pb corrections were calculated from ^{204}Pb measurements assuming an initial isotopic composition according to the Pb evolution curve of Stacey and Kramers (1975). Inter-element fractionation of Pb/U was generally ~20%, whereas fractionation of Pb isotopes is generally <2%. In-run analysis of fragments of a large zircon crystal (every fourth measurement) with a known age of 563.5 ± 3.2 Ma (2-sigma error, Gehrels *et al.*, 2008) was used to correct for this fractionation. The uncertainty resulting from the calibration correction is generally ~1% (2-sigma) for both $^{206}Pb/^{207}Pb$ and $^{206}Pb/^{238}U$ ages.

Sample 03-107 is a biotite and pyroxene tonalite from the Bacanora batholith, whose chemical analysis is shown in Table 1. Sample 03-11, from the San Lucas porphyry, was taken from a quartz monzonite dike with biotite and hornblende hosted by skarns and banded hornfels. Dating results are shown in Figure 3 and in Table 2. Sample 03-107 has a weighted mean $^{206}Pb/^{238}U$ age of 90.6 ± 1.0 Ma and sample 03-11 has a weighted mean $^{206}Pb/^{238}U$ age of 88.7 ± 1.0 Ma. No inherited component was recognized in the 52 grains analyzed in cores and tips. The systematic error (age of standard, calibration correction from standard, composition of common Pb, decay constant uncertainty) during the session was 1.1% and was added quadratically to the random errors of 0.4 and 0.3 % to assign uncertainties to the age determinations. These Late Cretaceous ages are interpreted as crystallization ages of these rocks, and correspond to the beginning of the magmatic Laramide event. Previous work in the area reported a K-Ar age in whole rock of 53 Ma for an intrusive body located west of the town of Bacanora (no coordinates reported), and a second age of 64 Ma (whole rock) from the Sierra Chiltepin (Pubellier, 1987). These ages are more typical of the Sonoran batholith (Damon *et al.*, 1981, 1983b), but it is likely that these K-Ar ages results are reset ages.

Geochemistry of the Bacanora batholith and the San Lucas porphyry

Samples from the Bacanora batholith and the San Lucas porphyry were selected for geochemical analysis at the geochemistry laboratory of the Centre des Recherches Pétrographiques et Géochimiques (CRPG) in Nancy, France. Samples were analyzed by ICP-MS following the procedure described by González-Partida *et al.* (2003a). Results are shown in the Table 1 and some typical diagrams are shown in Figures 4-7. Also, some summarized geochemical data from the Central Sonora batholith and Coastal Sonora batholith (Valencia-Moreno *et al.*, 1999, 2001, 2003) are shown for comparison in the same figures.

Table 1. Geochemical data for the Sierra Santo Niño rocks. Analysis performed at the Centre de Recherches Pétrographiques et Géochimiques de Nancy, France. Bb: Bacanora batholith, SLp: San Lucas porphyry.

		Bb 03-107	**Bb 03-108**	**Bb 03-110**	**Bb 03-100**	**Bb 03-101**	**Bb 03-103**	**SLp P03-80**	**SLp P03-83**	**SLp P03-92**	**SLp P03-117**	**SLp P03-118**
SiO_2	%	55.06	67.06	66.47	69.11	61.61	71.07	67.88	64.33	63.10	65.60	65.79
Al_2O_3	%	16.33	15.30	15.77	14.76	16.90	15.29	15.33	15.58	15.68	15.72	16.03
Fe_2O_3	%	7.42	3.43	3.60	3.76	5.61	2.27	2.71	3.35	4.27	2.58	1.09
MnO	%	0.12	0.03	N.D.	0.05	0.06	0.06	N.D.	0.04	0.04	N.D.	N.D.
MgO	%	4.82	2.00	1.24	0.98	2.64	N.D.	0.91	1.88	2.03	1.74	1.92
CaO	%	7.51	3.15	2.60	2.79	4.87	1.61	1.78	2.15	2.29	1.82	2.55
Na_2O	%	4.87	3.90	4.58	3.28	3.46	5.43	5.10	4.19	4.79	3.94	5.29
K2O	%	2.10	3.77	4.23	4.02	2.69	3.10	4.64	5.19	3.89	6.81	5.06
TiO_2	%	0.72	0.45	0.46	0.52	0.62	0.23	0.40	0.46	0.51	0.43	0.49
P_2O_5	%	0.24	0.14	0.13	0.12	0.19	0.06	0.13	0.15	0.21	0.16	0.17
LOI	%	0.74	0.72	0.85	0.50	1.28	0.50	1.06	2.70	3.10	1.14	1.51
Total	%	99.93	99.95	99.93	99.89	99.93	99.62	99.94	100.02	99.91	99.94	99.90
As	ppm	4.16	2.81	5.08	4.92	3.80	2.31	27.91	3.45	5.06	5.88	5.58
Ba	ppm	567.6	1007.0	1083.0	949.9	683.8	620.5	908.5	2264.0	1235.0	1726.0	957.0
Be	ppm	1.41	1.60	2.43	1.40	1.23	3.04	1.92	1.40	1.31	1.52	1.97
Bi	ppm	N.D.	0.73	N.D.	0.22	N.D.	0.26	2.01	N.D.	N.D.	N.D.	0.26
Ce	ppm	44.61	43.71	67.59	59.67	46.12	43.32	77.08	44.76	47.62	41.92	53.75
Co	ppm	22.87	9.88	6.89	7.37	13.42	1.94	34.46	8.54	8.90	5.58	3.71
Cr	ppm	91.56	75.90	23.75	8.16	16.91	N.D.	23.13	62.88	59.39	58.08	78.95
Cs	ppm	1.61	2.09	1.63	5.61	9.59	7.12	1.10	1.35	1.51	0.97	0.52
Cu	ppm	15.02	105.80	19.61	18.78	309.30	N.D.	519.20	N.D.	N.D.	N.D.	46.39
Dy	ppm	2.57	1.60	2.74	3.39	2.75	1.30	2.57	1.55	1.65	1.59	1.60
Er	ppm	1.43	0.84	1.48	1.72	1.38	0.90	1.39	0.76	0.79	0.78	0.85
Eu	ppm	1.05	0.78	0.98	0.92	1.05	0.53	0.96	0.91	0.94	0.82	0.72
Ga	ppm	19.43	18.49	19.86	17.45	19.17	17.82	16.15	19.88	19.62	19.12	19.30
Gd	ppm	2.99	2.06	3.38	3.96	3.28	1.42	3.22	2.21	2.44	2.34	2.14
Ge	ppm	1.37	1.12	1.24	1.26	1.40	1.67	0.94	0.79	0.90	1.07	1.03
Hf	ppm	3.50	3.91	5.66	5.90	3.61	5.97	5.44	3.10	3.35	3.13	4.31
Ho	ppm	0.51	0.30	0.52	0.62	0.50	0.27	0.48	0.28	0.29	0.29	0.30
La	ppm	22.88	24.42	34.91	29.55	22.78	26.23	43.25	22.60	25.12	19.50	22.40
Lu	ppm	0.24	0.15	0.26	0.26	0.22	0.24	0.24	0.12	0.12	0.13	0.16
Mo	ppm	0.71	0.60	0.78	0.85	0.76	N.D.	2.85	N.D.	1.21	N.D.	N.D.
Nb	ppm	6.55	8.11	11.02	9.61	6.66	10.22	12.01	6.97	7.01	8.14	8.35
Nd	ppm	19.22	16.61	27.60	24.93	20.23	11.69	27.11	19.26	20.22	19.08	20.25
Ni	ppm	25.10	30.46	13.02	5.39	11.18	N.D.	24.01	35.90	29.81	28.85	28.86
Pb	ppm	8.44	11.18	11.90	17.54	6.96	12.05	7.79	3.86	2.40	2.03	7.92
Pr	ppm	5.13	4.72	7.71	6.79	5.39	3.95	7.99	5.17	5.34	5.12	6.02
Rb	ppm	57.7	106.1	122.3	144.6	121.6	231.7	117.9	133.9	115.2	187.9	118.8
Sb	ppm	0.69	0.53	0.84	0.63	0.62	0.76	4.50	1.99	4.57	1.54	1.73
Sm	ppm	3.59	2.84	4.57	4.85	3.95	1.71	4.39	3.16	3.45	3.24	2.94
Sn	ppm	0.76	0.99	1.06	1.22	1.48	2.00	1.29	0.71	0.82	0.83	0.79
Sr	ppm	650.7	606.2	640.7	260.3	431.5	259.3	335.7	244.8	208.1	156.4	200.9
Ta	ppm	0.54	0.91	1.16	1.06	0.79	0.87	1.26	0.67	0.61	0.85	0.88
Tb	ppm	0.44	0.29	0.49	0.60	0.49	0.21	0.46	0.29	0.32	0.30	0.29
Th	ppm	5.96	12.63	16.42	20.85	16.52	13.43	17.71	8.42	7.34	9.97	12.52
Tm	ppm	0.22	0.13	0.24	0.25	0.21	0.16	0.21	0.11	0.11	0.12	0.14
U	ppm	2.44	5.82	4.44	5.83	5.73	5.59	8.04	4.07	4.04	4.72	7.04
V	ppm	179.20	67.18	67.93	71.89	124.50	15.96	58.17	68.53	72.30	63.25	85.80
W	ppm	0.44	1.01	0.76	1.33	2.38	0.37	1.76	1.46	2.68	2.23	1.96
Y	ppm	14.74	8.76	15.86	18.40	15.25	9.68	14.68	8.01	8.44	8.68	9.10
Yb	ppm	1.50	0.92	1.69	1.70	1.41	1.33	1.49	0.75	0.75	0.81	0.95
Zn	ppm	64.17	27.60	30.24	62.38	50.17	25.60	44.80	46.18	38.66	29.56	14.38
Zr	ppm	145.20	142.3	221.7	220.9	129.4	214.8	207.5	116.8	127.6	115.9	161.1

N.D.= Not detected; LOI= Loss on ignition.

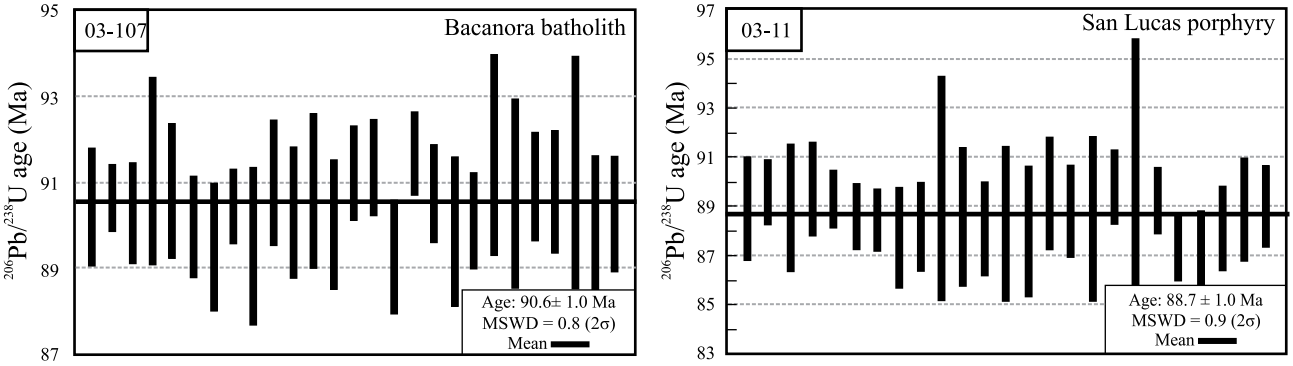

Figure 3. U-Pb zircon ages for the Bacanora batholith (03-107) and the San Lucas porphyry (03-11).

Six samples from the Bacanora batholith show that the SiO_2 range content is 55–71 % and the major oxides Al_2O_3, CaO, MgO, TiO_2 and P_2O_5 decrease systematically with increasing SiO_2 in Harker diagrams (Figure 4), whereas there are a good positive correlation between SiO_2 versus K_2O. Highest values in CaO corresponds to the tonalitic petrographic facies and high content in MgO and TiO_2 is consistent in samples with more abundant ferromagnesian minerals. The rocks plot in the high K calc-alkaline field in the K_2O/SiO_2 diagram (Figure 5). According to La Roche's *et al.* (1980) classification all rocks, excepting one, plot in the granodiorite, tonalite, quartz monzonite and syenogranite fields. The behavior of some key trace elements such as Sr/Rb versus SiO_2, which agrees with the degree of magmatic differentiation, suggest that these rocks originated from the same magma. A multi-element spider diagram shows a homogeneous behavior for the Bacanora batholith (Figure 6). In a REE plot, a LREE enrichment and a relative depletion in HREE is observed, followed by a very flat trend in the Dy-Lu segment (Figure 7). The $(La/Yb)_N$ is 9.6 and no Eu anomaly is present.

For the San Lucas porphyry five rock samples were analyzed. The samples have very similar characteristics because they come from an homogeneous individual stock that is classified as a hypabysal to subvolcanic quartz monzonite. The geochemical analysis are shown in Table 1 and some average values are included in Table 3. The SiO_2 composition is restricted to 63–68 % and the most important chemical differences with respect to the Bacanora batholith is the enrichment in K_2O and depletion in CaO at similar SiO_2 values. The high K_2O average concentration (5.1 %), is due to the presence of K-feldspar in the rock matrix; low CaO concentrations are due to the mainly sodic composition (An<30) of plagioclase that is only present as phenocrysts. The San Lucas porphyry compositions generally plot in the shoshonite field (Figure 5). The rock is Fe_2O_3 and MgO poor, as biotite and hornblende are in low abundance. Depletion of MgO, TiO_2 and P_2O_5 occurs as SiO_2 increases. The porphyry composition plots within the quartz monzonite field according to La Roche's *et al.* (1980) classification. The characteristic mean content of trace elements is given in Table 3. Sr is in general depleted and exhibits an inverse behavior to K_2O, suggesting that plagioclase controls the Sr content (plagioclase decreases as K-feldspar increases). Ni and Cr concentrations are higher than in volcanic arc granodiorite (Table 3) compiled by Martin (1999), while Y and Yb concentrations are lower. As in the Bacanora batholith, the REE pattern shows a LREE enrichment and a HREE depletion ($(La/Yb)_N > 10$), with no Eu anomaly present.

In summary, geochemistry of major and some trace elements of the Bacanora batholith and of the San Lucas porphyry could be explained by mineralogical composition. The basic differences are in high K_2O, low CaO and restricted SiO_2 for the San Lucas porphyry, and different concentrations for Ba, Pb and Sr in the multi-element diagram (Figure 6); the REE patterns in both cases are overlapped (Figure 7), suggesting an origin from the same magma source as it is discussed later. Field relations indicate that the Bacanora batholith (90.6 Ma) is intruded by the San Lucas porphyry (88.7 Ma). The similar age for both intrusive rocks suggest a comagmatic origin, being the San Lucas porphyry the latest intrusive facies, probably more contaminated by continental crust (higher in K_2O).

Relation of the Bacanora batholith and the San Lucas porphyry with adakites

As defined by Defant and Drummond (1990), adakites are intermediate to acidic rocks, and include andesites, dacites and rhyolites. They are porphyritic lavas containing zoned plagioclase, biotite, hornblende and rarely pyroxene. Their general silica content is >56%, Al_2O_3 >15 %, Na_2O 3.5–7.5% and K_2O/Na_2O ~0.42. Key discriminants for adakites are: $(La/Yb)_N$ *versus* Yb_N (Martin, 1987, 1999) and Sr/Yb *versus* Y (Defant and Drummond, 1990). Adakites are similar to the calc-alkaline series, but they generate in particular collisional geotectonic environments and have been interpreted as originated from the partial melting of a subducted oceanic slab that interacts with the mantle wedge (Martin *et al.*, 2005).

In relation with key discriminant elements, the San

Table 2. Individual U-Pb ages on zircons for the Bacanora batholith (sample 03-107) and the San Lucas porphyry (sample 03-11).

	U (ppm)	Th (ppm)	U/Th	$^{206}Pb/^{204}Pbc$	$^{206}Pb/^{238}U$ ratio	±(%)	$^{206}Pb/^{238}U$ age	±(Ma)
Sample 03-107								
1	375	180	2.1	832	0.01412	1.54	90.4	1.4
2	569	600	0.9	1409	0.01416	0.88	90.6	0.8
3	250	201	1.2	701	0.01410	1.31	90.3	1.2
4	192	110	1.7	517	0.01425	2.38	91.2	2.2
5	394	316	1.2	807	0.01418	1.73	90.8	1.6
6	336	203	1.7	775	0.01405	1.33	89.9	1.2
7	275	131	2.1	735	0.01398	1.66	89.5	1.5
8	560	437	1.3	1484	0.01413	0.95	90.4	0.9
9	317	228	1.4	667	0.01398	2.06	89.5	1.8
10	513	336	1.5	1565	0.01421	1.61	91.0	1.5
11	246	143	1.7	1075	0.01410	1.72	90.3	1.5
12	184	127	1.4	667	0.01419	1.97	90.8	1.8
13	287	143	2.0	1236	0.01406	1.67	90.0	1.5
14	375	220	1.7	1061	0.01425	1.21	91.2	1.1
15	480	467	1.0	1083	0.01427	1.23	91.3	1.1
16	340	261	1.3	397	0.01394	1.49	89.2	1.3
17	459	237	1.9	1047	0.01432	1.07	91.6	1.0
18	266	222	1.2	1137	0.01417	1.26	90.7	1.1
19	188	90	2.1	1161	0.01403	1.93	89.8	1.7
20	231	183	1.3	817	0.01408	1.25	90.1	1.1
21	146	73	2.0	368	0.01432	2.55	91.6	2.3
22	156	83	1.9	442	0.01412	2.81	90.4	2.5
23	523	423	1.2	2559	0.01420	1.41	90.9	1.3
24	261	213	1.2	746	0.01418	1.57	90.8	1.4
25	133	75	1.8	450	0.01418	3.43	90.8	3.1
26	275	174	1.6	1548	0.01405	1.84	89.9	1.6
27	223	124	1.8	1519	0.01410	1.51	90.2	1.4
Sample 03-11								
1	404	207	2.0	873	0.01388	2.36	88.9	2.1
2	398	178	2.2	1463	0.01399	1.43	89.6	1.3
3	335	106	3.2	1277	0.01391	2.92	89.0	2.6
4	509	248	2.1	1488	0.01402	2.12	89.7	1.9
5	602	289	2.1	1413	0.01395	1.30	89.3	1.2
6	1238	1146	1.1	5555	0.01384	1.51	88.6	1.3
7	673	252	2.7	3535	0.01382	1.42	88.5	1.2
8	314	272	1.2	1292	0.01370	2.35	87.7	2.1
9	543	238	2.3	1481	0.01377	2.03	88.2	1.8
10	193	95	2.0	1170	0.01402	5.03	89.8	4.5
11	360	147	2.5	1197	0.01384	3.14	88.6	2.8
12	422	476	0.9	1875	0.01376	2.22	88.1	1.9
13	176	83	2.1	535	0.01379	3.50	88.3	3.1
14	328	148	2.2	510	0.01375	2.95	88.0	2.6
15	402	209	1.9	2151	0.01398	2.51	89.5	2.2
16	435	266	1.6	2688	0.01387	2.10	88.8	1.9
17	196	99	2.0	847	0.01383	3.73	88.5	3.3
18	474	224	2.1	2148	0.01403	1.66	89.8	1.5
19	156	93	1.7	969	0.01412	5.98	90.4	5.4
20	598	419	1.4	2568	0.01394	1.52	89.2	1.3
21	387	195	2.0	807	0.01364	1.49	87.3	1.3
22	455	204	2.2	2322	0.01363	1.82	87.3	1.6
23	385	196	2.0	1475	0.01376	1.96	88.1	1.7
24	456	237	1.9	1498	0.01389	2.33	88.9	2.1
25	346	184	1.9	2167	0.01391	1.83	89.0	1.6

Lucas porphyry has a low Sr concentration (229 ppm in average), whereas the Bacanora batholith rocks have an average of 475 ppm Sr; this element is controlled by feldspars proportion in the rocks. In the Sr/Y *vs.* Y and $(La/Yb)_N$ *vs.* Yb_N diagrams, these rocks plot within or near the adakite field (Figure 8). From the multi-element diagram and REE plots, a similar pattern is observed for the Bacanora batholith and the San Lucas porphyry, which also supports a common origin (Figures 7 and 8), with an LREE enrichment and a HREE depletion and with $(La/Yb)_N > 9.7–14.1$. The HREE

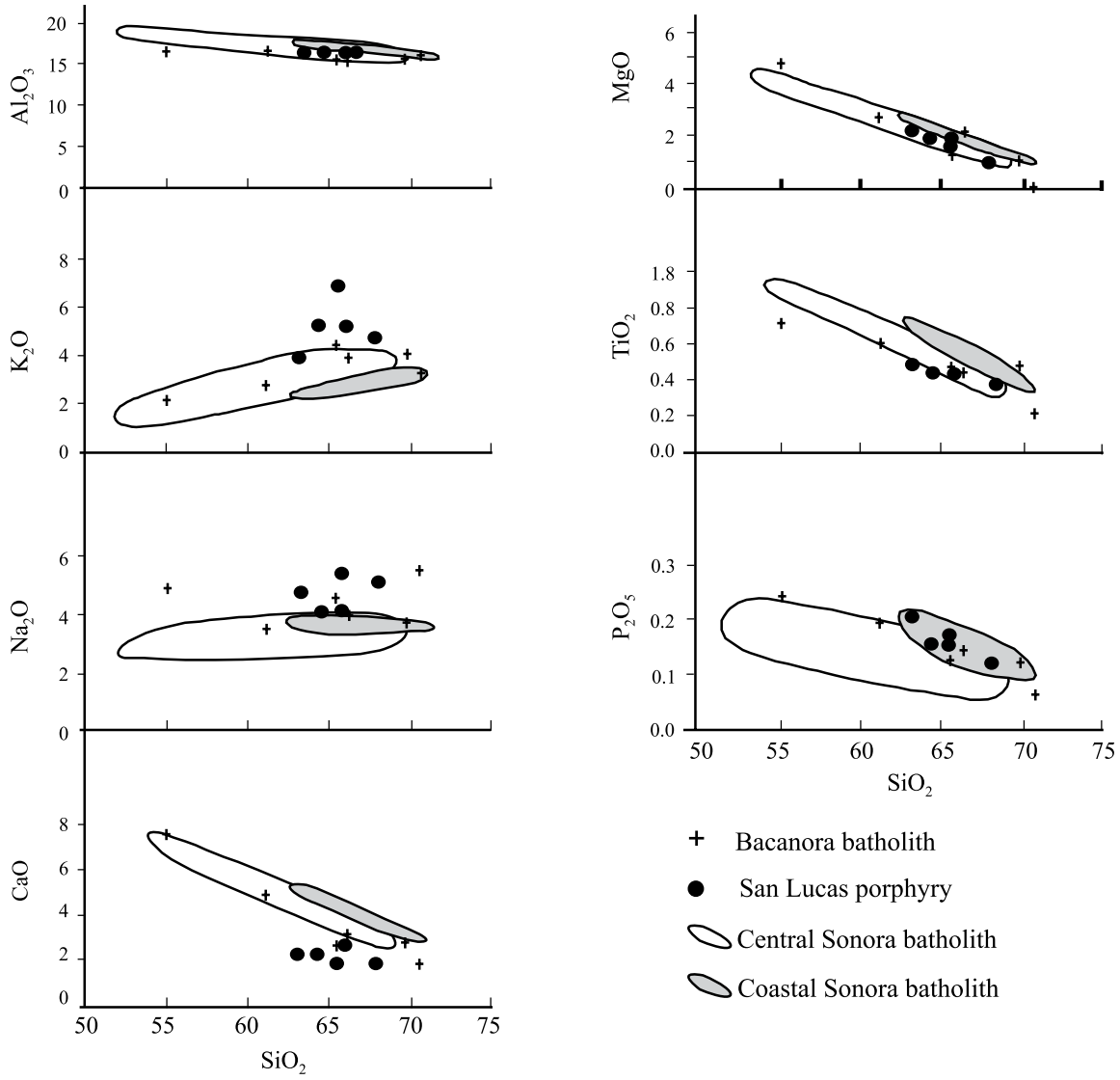

Figure 4. Harker diagrams for the studied rocks, and fields composition for Central Sonora batholith (42-46 analyses) and Coastal Sonora batholith (16 analyses). Analysis from Central and Coastal Sonora batholith from Valencia-Moreno *et al.* (1999, 2001, 2003) and Roldán-Quintana (2002).

depletion can be interpreted as reflecting the presence of garnet + hornblende in the restite of the magma source (Martin, 1999). However, the Ni values (>24 ppm) and Cr (>36 ppm) values in the San Lucas porphyry are higher than typical adakites, which can be interpreted as an adakitic magma reacting with the peridotitic mantle wedge (Maury *et al.*, 1996; Martin, 1999; Martin *et al.*, 2005). The most important argument supporting a co-magmatic origin for the Bacanora batholith and the San Lucas porphyry are the similar crystallization ages (~90 Ma).

DISCUSSION AND CONCLUSIONS

The emplacement of the Sonoran batholith (90–40 Ma) has been proposed as occurring in belts parallel to the Pacific coast, with progressively younger ages inland (Damon *et al.* 1981; Clark *et al.*, 1979, 1982). Table 4 shows a selected compilation of published Laramide rocks ages in Sonora, older than 62 Ma. Most of them are indicated in Figure 9. Numbers in brackets in Figure 9 and in Table 4 correspond to the localities mentioned in this text (in italics). Up to now the oldest ages reported for Laramide intrusive rocks in this region are near the coast. Ages of 82.7 Ma (K-Ar in hornblende) at Punta San Antonio (*11*) and 77 Ma (K-Ar in biotite) in Rancho El Bayo (*12*) have been reported by Mora-Alvarez and McDowell (2000). Gastil and Krummenacher (1977) reported K-Ar ages in biotite on rocks from the following places between Bahía Kino and Puerto Libertad: 91 Ma at Cerro Bolo (*6*), 85–90 Ma in Tiburón Island (*7*, *8*), 71.7 Ma at Punta Cuevas and 70.1 Ma in Puerto Libertad (*9*). On the other hand, Damon *et al.* (1983b) reported 70.9 Ma (K-Ar in biotite) at the Leones mine (near Puerto Libertad). More recent data published by

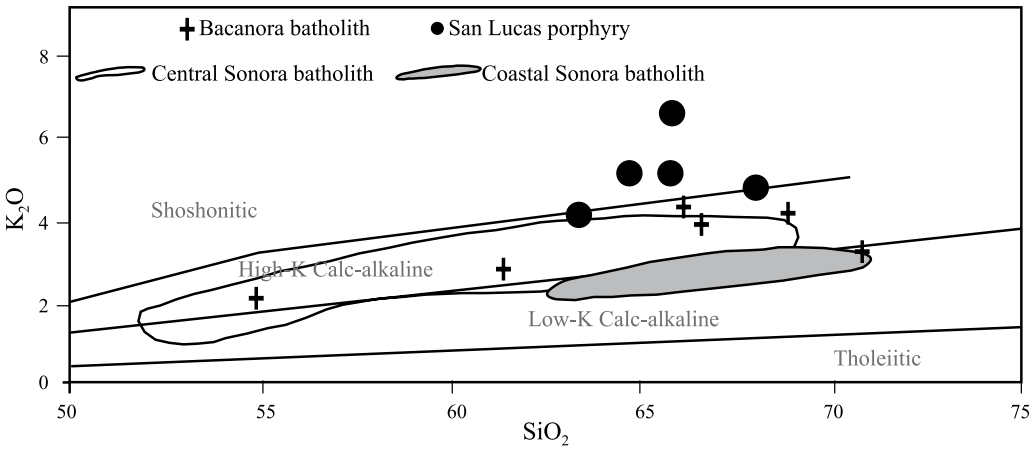

Figure 5. SiO_2 *vs.* K_2O diagram for the rocks studied compared with Central and Coastal Sonora batholith. The high-K, medium-K and low-K lines are according to Le Maitre *et al.* (1989). The high-K – shoshonite boundary is according to Rickwood (1989).

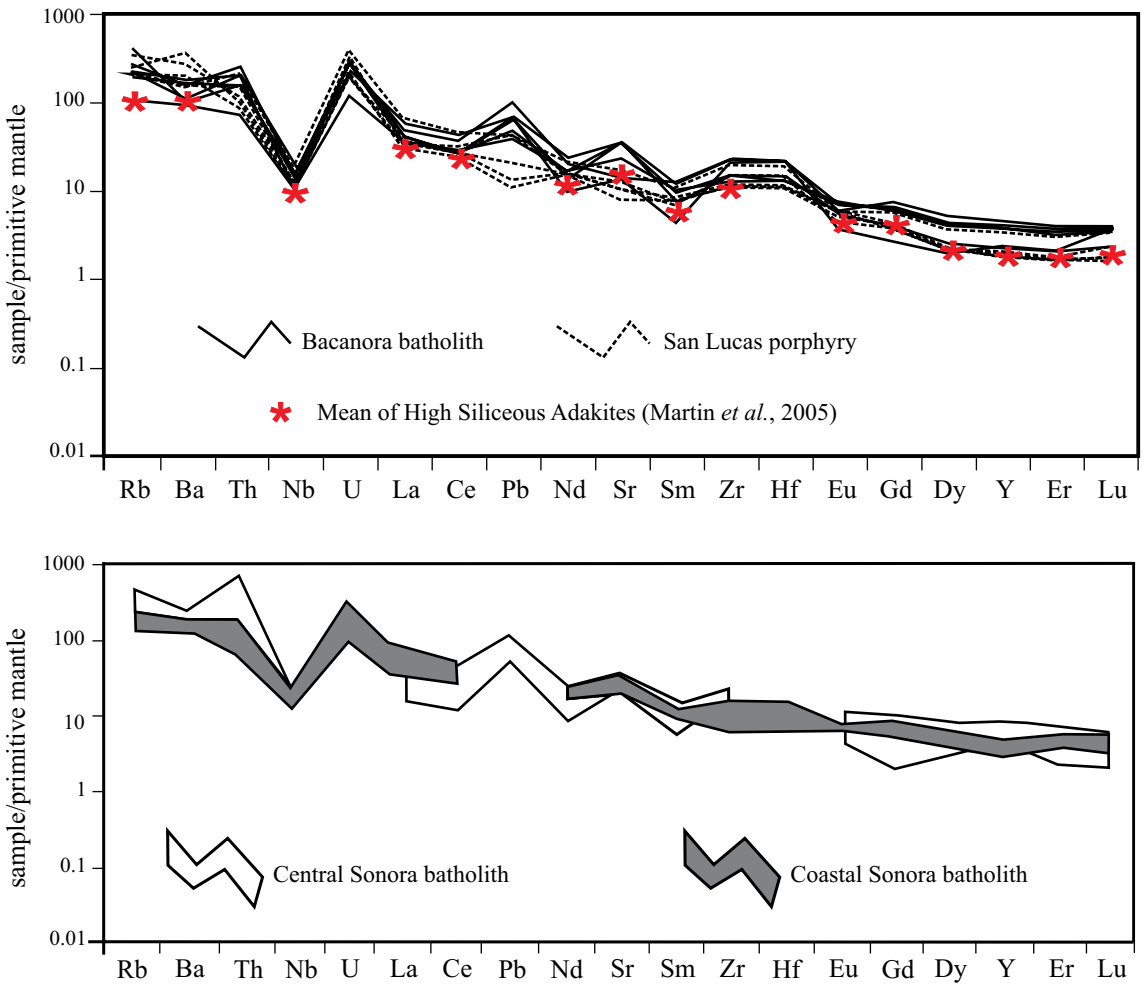

Figure 6. Multi-element diagram for the Bacanora batholith and San Lucas porphyry. Analysis normalized to primitive mantle (Hofmann, 1997). * Mean values of 767 analyses of High Siliceous Adakites – HSA (Martin *et al.*, 2005). Lower diagram: General behavior for the Central Sonora batholith and Coastal Sonora batholith using data from Valencia-Moreno *et al.* (1999, 2001, 2003), and Roldán-Quintana (2002).

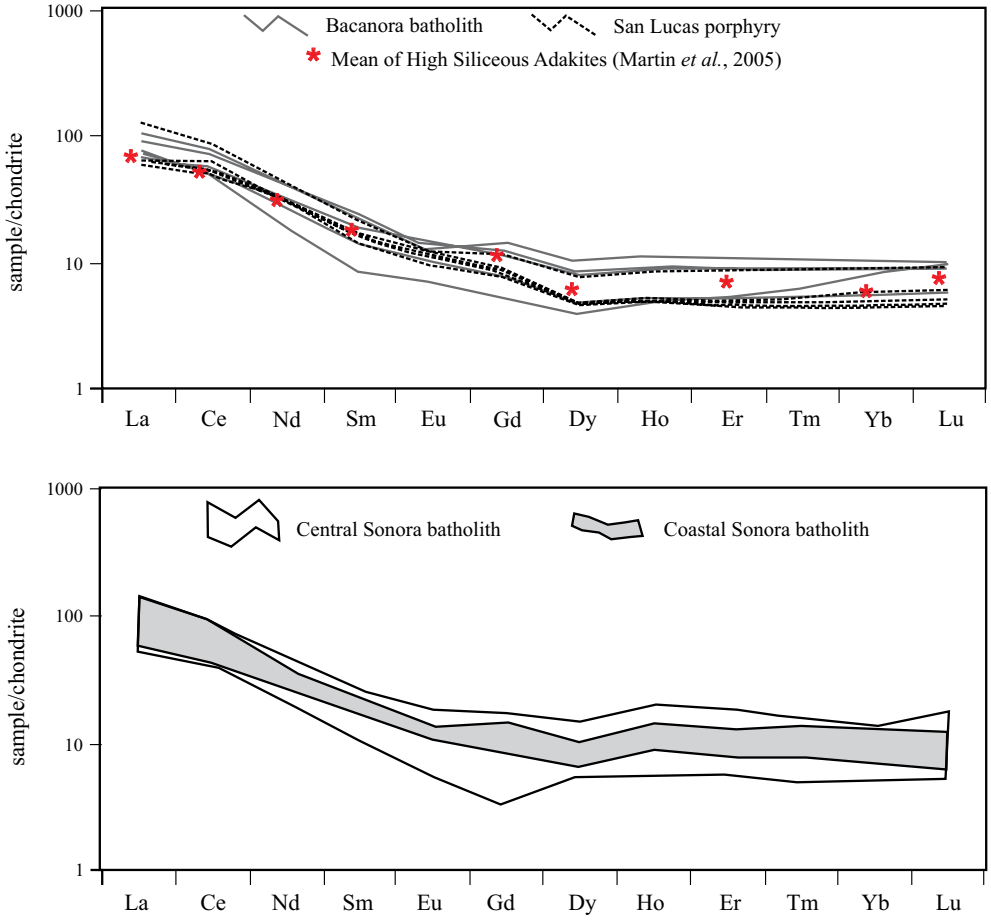

Figure 7. REE diagram for Bacanora batholith and the San Lucas porphyry samples. Analysis normalized to chondrite (Nakamura, 1974) * Mean values of 767 analyses of High Siliceous Adakites – HSA (Martin *et al*, 2005). Lower diagram: General behavior for the Central Sonora batholith and Coastal Sonora batholith, using data from Valencia *et al.* (2001), Roldán-Quintana (2002) and Valencia-Moreno *et al.* (2003) normalized to Nakamura (1974).

Ramos-Velázquez *et al.* (2008) include ages from 72 to 90 Ma (U-Pb in zircons) for granitoids between Bahía Kino and Punta Tepopa (localities *21-29*). Rocks ranging in age from 70 to 100 Ma (Ar/Ar) are more common in the Baja California Peninsula (Tulloch and Kimbrough, 2003) and in the state of Sinaloa (Henry *et al.*, 2003).

The U-Pb isotopic analysis in zircon for the Tarahumara Formation in the Tecoripa-Tónichi-La Dura-Suaqui Grande quadrangles (McDowell *et al.*, 2001) yielded ages in the range from 90.1 to 69.7 Ma. This formation is overlain by unaltered volcanic rocks, with ages of 62–53 Ma, that are not considered part of the Tarahumara Formation (Roldán-Quintana, 2002). Volcanic rocks of 90–60 Ma have been identified in different areas of Sonora, *e.g.*, Jacques-Ayala *et al.* (1993) report a 72 Ma age (K-Ar in hornblende) for andesites in the Sierra El Chanate (*19*); Gastil and Krummenacher (1977) dated a 85.1 Ma (K-Ar in hornblende) andesite and a 64 Ma (K-Ar in biotite) dacite at Puerto Libertad; Meinert (1982) reported ages of 67 Ma (K-Ar) for the Mesa Formation at Cananea (*20*) and Wodzicki (1995) obtained a 69 Ma (Ar/Ar in biotite) age for the same formation. At Arivechi, closer to our study area, Pubellier *et al.* (1995) found ages of 66 Ma and 75 Ma (K-Ar in whole rock) for andesites, and Pubellier (1987) reported a strongly potassic porphyritic andesite with an age of 83 Ma (K-Ar in whole rock).

The new U-Pb ages reported here show that the intrusive rocks of the Bacanora batholith, including the San Lucas porphyry, were emplaced as early as 90 Ma. Our geochronological data establish the oldest Late Cretaceous (Laramide) intrusive rocks in east-central Sonora, which intrude andesitic volcanic rocks that are older than the ones described by McDowell *et al.* (2001), about 50–75 km to the south of the study area. The age of thrusting of the Paleozoic platform strata over the pre-batholithic andesites is constrained to a period ranging from 100 Ma to 91 Ma; the limits are established in accordance with the evidence of the Bacanora batholith (91 Ma) and the San Lucas porphyry (90 Ma) intruding Paleozoic limestones and Cretaceous andesites; the oldest 100 Ma limit is fixed according to the thrusting of Neoproterozoic sedimentary rocks over Albian-Cenomanian limestones at Sierra Chiltepín, on the highway between Bacanora and Sahuaripa (Pubellier *et al.*, 1995).

Several authors (Damon *et al.*, 1981, 1983b; Valencia-

Table 3. Mean values for some key elements for the Sierra Santo Niño rocks and comparison with other adakitic rocks. Bb. Bacanora batholith, SLp. San Lucas porphyry.

Composition	Bb (6)	SLp (5)	Adakite[1]	Adakitic pluton[1]	Suite La Posta[2]	Mezcala[3]
SiO_2	65.06	65.34	64.66	67.3	67.79	64.14
Al_2O_3	15.72	15.67	16.77	15.78	15.68	15.92
Fe_2O_3	4.35	2.80	4.20	3.30	3.45	4.10
MnO	0.06	0.02	0.08	0.05	0.05	0.10
MgO	1.95	1.70	2.20	1.96	1.20	2.30
CaO	3.76	2.12	5.00	3.67	3.86	4.20
Na_2O	4.26	4.66	4.09	4.19	3.51	3.90
K_2O	3.32	5.12	1.72	2.15	2.57	3.30
TiO_2	0.50	0.46	0.51	0.54	0.62	0.70
P_2O_5	0.15	0.16	0.17	0.12	0.14	0.30
Fe_2O_3+MgO+MnO+TiO_2	6.8	5.0	7.0	5.8	5.3	7.2
K_2O/Na_2O	0.8	0.9	0.4	0.5	0.7	0.8
Sr	475.0	229	706.0	280.0	483.0	790.0
Ni	14.0	30.0	24.0	24.0	7.0	21.0
Cr	36.0	56.0	36.0	46.0	15.0	53.0
Y	12.5	10.0	10.0	17.0	9.0	13.0
Yb	1.3	0.9	0.9	1.1		1.1
Sr/Y	37.0	24.0	68.7	16.5	54.0	61.0
$(La/Yb)_N$	9.6	14.1	14.2	11.0	23.0	20.0

[1] Martin (1999); [2] Tulloch and Kimbrough (2003); [3] González-Partida *et al.* (2003a). (N)= number of analysis.

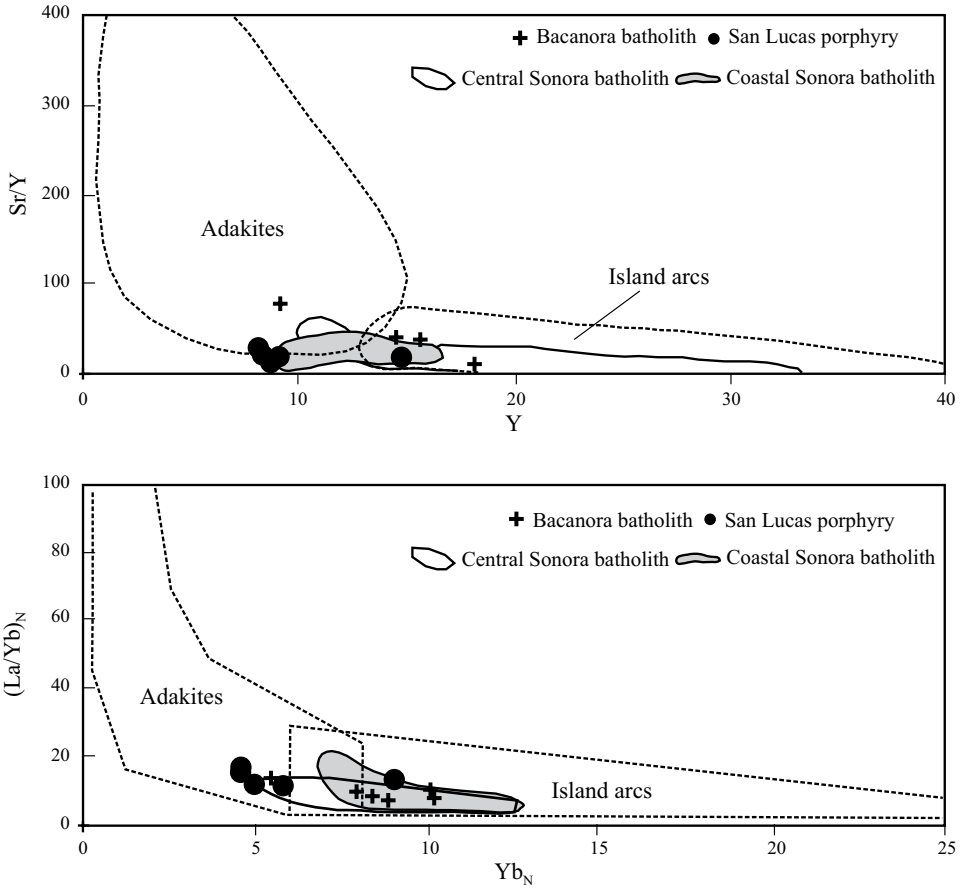

Figure 8. Data of the Bacanora batholith and the San Lucas porphyry ploted on the Sr/Y – Y (Drummond and Defant, 1990) and $(La/Yb)_N$ – Yb_N (Martin, 1987) diagrams. Fields corresponding to the Central Sonora batolith (16 analysis) and Coastal Sonora batholith (16 analysis) are also shown (same source of data as for Figure 7).

Table 4. Compilation of published radiometric ages for Late Cretaceous igneous rocks in Sonora, Mexico.

Sample	Location	Locality	Rock	Dated mineral	Method	Age	Ref.
UAKA80-07	28° 37', 109° 53' 18"	San Javier-Tecoripa	Granodiorite	Biotite	K/Ar	61.2 ± 1.3	1
				Hornblende	K/Ar	62.0 ± 1.7	1
UAKA80-18	27° 45', 109° 43'	Santa Ana	Granodiorite	Biotite	K/Ar	67.3 ± 1.4	1
				Hornblende	K/Ar	66.1 ± 1.4	1
(*1*) PED11-59	30° 40' 54", 112° 16' 30"	Puerto Blanco	Quartz monzonite	Biotite	K/Ar	71.2 ± 1.8	1
(*2*) PED7-59	30° 31' 50", 112° 07' 05"	Altar	Pegmatite	Biotite	K/Ar	74.3 ± 1.8	1
PED-10-66	31° 11' 42", 112° 17' 14"	Minas Leones Caborca	Granite	Biotite	K/Ar	70.9 ± 2.1	1
(*3*) PED-11-66	31° 08' 46", 112° 04' 56"	Minas Margarita Caborca	Granite	Biotite	K/Ar	67.6 ± 2	1
UAKA83-03	29° 21' 24", 109° 16' 24"	Sierra Oposura	Granodiorite	Biotite	K/Ar	62.7 ± 1.4	1
UAKA80-20	28° 50' 32", 110° 12' 20"	Cobachi	Granodiorite	Biotite	K/Ar	66.7 ± 1.6	1
UAKA81-01	28° 53' 06", 109° 48' 54"	Rebeico	Monzonite	Matrix	K/Ar	61.2 ± 1.4	1
UAKA80-05	28° 52' 18", 110° 45' 43"	Granito Hermita	Granodiorite	Hornblende	K/Ar	62.9 ± 1.5	1
Ma-1	NR	Maycoba	Granodiorite	Biotite	K/Ar	63.6 ± 1.0	2
(*4*) SO-36	641.55, 3140.10	La Dura	Porphyritic dacite	Zircon	U/Pb	66.2 ± 2.0	3
SO-64	591.25, 3140.45	18 km W Suaqui Grande	Granodiorite	Biotite	K/Ar	63.4 ± 1.0	4
SO-74	583.25, 3131.95	28 km SW Suaqui Grande	Quartz diorite	Biotite	K/Ar	64.9 ± 1.7	4
SO-2	606.65, 3165.65	3.5 km E Tecoripa	Granodiorite	Biotite	K/Ar	65.1 ± 1.0	4
SO-5	631.60, 3160.20	7.5 km SE San Javier	Quartz diorite	Hornblende	K/Ar	62.4 ± 2.5	4
MV-9	28° 36' 16", 110° 01' 14"	Cerro Bola	Granodiorite	Hornblende	K/Ar	62.0 ± 1.7	5
MV-10	28° 28' 27", 110° 28' 08"	San Francisco	Granodiorite	Hornblende	K/Ar	62.9 ± 1.5	5
MV-12	29° 06' 49", 110° 56' 19"	Hermosillo	Granodiorite	Hornblende	K/Ar	64.1 ± 1.4	5
MV-14	29° 05' 02", 110° 56'10"	Hermosillo	Granodiorite	Hornblende	K/Ar	64.1 ± 1.4	5
MV-15	29° 03' 00", 110° 56' 56"	Hermosillo	Granodiorite	Hornblende	K/Ar	64.1 ± 1.4	5
(*5*) NR	30° 58' 54", 111° 02' 48"	Sierra Guacomea	Granite/gneiss	Zircon	U/Pb	78.3 ± 3	6
MV-19	28° 53' 51", 109° 54' 16"	Barita de Sonora	Granite	Zircon	U/Pb	62.0 ± 1	7
NR	NR	Tiburon Island	Tonalite	Biot-Whole rock	Rb/Sr	82	8
NR	29° 03' 36", 110° 56' 42"	Carnaval, Hermosillo	Granodiorite	Biotite	Ar/Ar	64.9 ± 1.3	9
WAKA81-06	29° 05' 20", 110° 56' 08"	Mariachi, Hermosillo	Granodiorite	Hornblende	Ar/Ar	64.1 ± 1.4	9
TP-2B	28° 25' 109° 11'	Tres Piedras, Santa Rosa	Granodiorite porphyry	Hornblende	Ar/Ar	63.3 ± 3.3	9
B-59	30° 40', 119° 16'	Sierra Manzanal	Granodiorite	Biotite	Ar/Ar	68	11
NR	NR	Pitiquito	Granite	NR	K/Ar	80	12
NR	NR	Cuitaca Cananea	Granodiorite	Zircon	U/Pb	64 ± 3	15
NR	NR	Chivato Cananea	Monzodiorite	Zircon	U/Pb	69 ± 1	15
S1G-6	29° 54' 10", 112° 43' 35"	Cerro Bolo Costa Sonora	Granodiorite	Hornblende	K/Ar	60.9 ± 9.9	16
(*6*) S1G-6	29° 54' 10", 112° 43' 35"	Cerro Bolo Costa Sonora	Granodiorite	Biotite	K/Ar	91.0 ± 1.8	16
(*7*) S2R-19	29° 12' 45", 112° 27' 45"	NW Tiburon Island	Tonalite	Hornblende	K/Ar	84.5 ± 7.9	16
(*7*) S2R-19	29° 12' 45", 112° 27' 45"	NW Tiburon Island	Tonalite	Biotite	K/Ar	85.2 ± 1.7	16
(*8*) S2W-45	29° 05' 50", 112° 19' 35"	NE Tiburon Island	Tonalite	Hornblende	K/Ar	90.4 ± 2.7	16
(*8*) S2W-45	29° 05' 50", 112° 19' 35"	NE Tiburon Island	Tonalite	Biotite	K/Ar	81.5 ± 2.0	16
S2G-23	29° 08', 111° 54'	E Noriega Creek	Granite	Microcline	K/Ar	64.7 ± 1.3	16
S0H-281	29° 42' 00", 112° 32' 30"	Cuevas Point	Granodiorite	Biotite	K/Ar	71.7 ± 1.4	16
(*9*) S0K-3714	29° 57' 45", 112° 44' 55"	N Puerto Libertad	Granodiorite porphyry	Biotite	K/Ar	70.1 ± 1.9	16
S0K-3714	29° 57' 45", 112° 44' 55"	N Puerto Libertad	Granodiorite porphyry	Hornblende	K/Ar	64.3 ± 2.0	16
CR H 12	NR	Sierra Chiltepin	Granitoid	Whole rock	K/Ar	63.6 ± 3.2	17
M-120	NR	Milpillas	Quartz monzonite porphyry	Zircon	U/Pb	63.9 ± 2.0	18
M-098	NR	Milpillas	Molybdenite	Molybdenite	Re/Os	63.1 ± 0.3	18
(*10*) M-120	NR	Milpillas	Molybdenite	Molybdenite	Re/Os	63.0 ± 0.3	18
(*11*) SO-25	487.55, 3094.65	Norte San Carlos	Granodiorite	Biotite	K/Ar	81.1 ± 2.8	19
				Hornblende	K/Ar	82.7 ± 1.7	19
(*12*) SO-59	502.50, 3121.3	R.El Bayo, Guaymas	Granodiorite	Biotite	K/Ar	76.9 ± 2.8	19
SO-59	502.50, 3121.3	R.El Bayo, Guaymas	Granodiorite	Zircon	U/Pb	78 ± 2	19
(*22*) KI-12-46	365 796, 3247 634	Bahía Kino – Punta Tepopa	Tonalita	Zircon	U/Pb	69.4	20
(*23*) KI-12-41	380 900, 3244 078	Bahía Kino – Punta Tepopa	Tonalita	Zircon	U/Pb	72.0	20
(*24*) KI-12-35	387 066, 3238 468	Bahía Kino – Punta Tepopa	Granite	Zircon	U/Pb	75.9	20
(*25*) KI-12-53	387 368, 3214 508	Bahía Kino – Punta Tepopa	Tonalite	Zircon	U/Pb	70.8	20
(*26*) KI-12-12	391 513, 3209 999	Bahía Kino – Punta Tepopa	Granodiorite	Zircon	U/Pb	81.4	20
(*27*) KI-03-15	408 084, 3202 328	Bahía Kino – Punta Tepopa	Granodiorita	Zircon	U/Pb	90.1	20
(*28*) KI-03-03	402 750, 3198 692	Bahía Kino – Punta Tepopa	Granite	Zircon	U/Pb	74.0	20
(*29*) KI-03-07	399 405, 3194 133	Bahía Kino – Punta Tepopa	Granodiorite	Zircon	U/Pb	84.1	20

Table 4. (Continued).

Sample	Location	Locality	Rock	Dated mineral	Method	Age	Ref.
SO-51	643.90, 3142.50	5 km NE La Dura	Porphyrytic dacite	Feldspar	K/Ar	62.5 ± 1.5	4
SO-97	686.97, 3142.44	Santa Ana, Yécora	Altered andesite	Plagioclase	K/Ar	61.2 ± 3.4	4
(*13*) 1	28° 20', 109° 58'	10 km W Suaqui	Tuff	Zircon	U/Pb	90.1 ± 0.7	10
(*14*) 2	28° 20', 109° 48'	10 km E-SE Suaqui	Crystal tuff	Zircon	U/Pb	89.0 ± 0.8	10
(*15*) 3	28° 20', 109° 46'	10 km E-SE Suaqui	Crystal tuff	Zircon	U/Pb	70.2 ± 0.6	10
(*16*) 4	28° 30', 109° 38'	10 km NW Onavas	Crystal tuff	Zircon	U/Pb	72.5 ± 0.5	10
(*17*) 5	28° 30', 109° 37'	10 km NW Onavas	Ignimbrite	Zircon	U/Pb	69.7 ± 0.6	10
(*18*) 6	28° 30', 109° 26'	10 km NE Onavas	Tuff	Zircon	U/Pb	72.6 ± 0.8	10
(*19*) NR	NR	Sierra El Chanate	Andesite	Hornblende	Ar/Ar	71.6 ± 0.7	12
(*20*) NR	NR	Cananea	La Mesa Fm	NR	K/Ar	67.4 ± 3.4	13
(*20*) NR	NR	Cananea	La Mesa Fm	Biotite	Ar/Ar	69.0 ± 0.2	14
(*21*) S1G-5	28° 52' 20'', 112° 01' 50''	NW Bahía Kino	Hornblende andesite	Hornblende	K/Ar	85.1 ± 1.7	16
S0K-276	29° 54' 55'', 112° 54' 55''	N Puerto Libertad	Dacitic porphyry	Biotite	K/Ar	63.9 ± 2.0	16
CR I 25	NR	4.5 km SE Arivechi	Andesite	Whole rock	K/Ar	65.7 ± 3.3	17
CR I 25	NR	4.5 km SE Arivechi	Andesite	Whole rock	K/Ar	65.9 ± 3.3	17
CRM 0	NR	4 km SE Arivechi	Andesite	Whole rock	K/Ar	73.8 ± 3.7	17
CRM 0	NR	4 km SE Arivechi	Andesite	Whole rock	K/Ar	74.6 ± 3.7	17
A-1	NR	La Caridad	Andesite	Zircon	U/Pb	64.2 ± 2.5	18

References: 1. Damon *et al.* (1983a, 1983b, 1986); 2. McDowell (*in* Bockoven, 1980); 3. Mc Dowell and Roldán-Quintana (1993 9; 4. McDowell (*in* Roldán-Quintana, 2002); 5. Damon *et al.* (1983); 6. Anderson *et al.* (1980); 7. Poole *et al.* (1991); 8. Schaaf *et al.* (1999); 9. Mead *et al.* (1988); 10. Mc Dowell *et al.* (2001), 11. González-León *et al.* (2000); 12. Jacques-Ayala *et al.* (1993); 13. Meinert (1982); 14. Wodzicki (1995); 15. Anderson and Silver (1977); 16. Gastil and Krummenacher (1977); 17. Pubellier *et al.* (1995); 18. Valencia-Gómez (2005); 19. Mora-Alvarez and McDowell (2000); 20. Ramos-Velázquez *et al.* (2008). Note: Coordinates in location as they are reported in the references. Numbers in italics are refered to the text and Figure 9.

Moreno *et al.*, 2001, 2003; Roldán-Quintana, 2002) have pointed out the calc-alkaline nature of the Sonoran batholith. In general, the rocks of the Sonoran batholith have higher Y and Yb_N values than the Bacanora batholith and the San Lucas porphyry, and plot mainly in the island arcs fields of the Drummond and Defand (1990) and Martin (1987) diagrams. The HREE values of the Sonoran batholith are less depleted compared to the analysis reported here for the Bacanora batholith and the San Lucas porphyry (Figure 7). The Sr isotopic data indicate $^{87}Sr/^{86}Sr$ ratios higher than 0.707 for the northern and central Sonora granitoids (Damon *et al.*, 1983b; Valencia-Moreno *et al.*, 1999, 2001), which have been interpreted as reflecting a continental crust contribution to the magmas (Valencia-Moreno *et al*, 2001).

The intrusive rocks of the Sierra Santo Niño (Bacanora batholith and San Lucas porphyry) have an adakitic signature and hence were probably generated by the partial melting of an eclogitic oceanic slab with garnet + amphibole in the restite. This melt may have reacted with the overlying peridotitic mantle wedge to produce the Cr and Ni anomalies observed in granitoid rocks and at the La Esperanza skarn deposits (Pérez-Segura *et al.*, 2004). Other adakitic intrusive rocks that have been described in México include the Paleocene intrusions reported in Mezcala, Guerrero (González-Partida *et al.*, 2003a, 2003b). Tullock and Krimbrough (2003) have also proposed a "high Sr/Y plutonic magmatism", which could be look like adakites in Baja California (La Posta suite), composed of hornblende + biotite bearing granitoids with ages between 99 and 92 Ma (Ar/Ar).

Defant and Drummond (1990) and Drummond and Defant (1990) proposed that adakitic magma formation requires the subduction of a young (<25 Ma) and hot oceanic crust, which does not fit in early Laramide geodynamic setting for this portion of North America. In contrast, some authors (Maury *et al.*, 1996) have indicated that adakites can be considered as geodynamic markers for the interaction of young oceanic crust subducted underneath a continental plate. Thus, adakites appear to be linked to the beginning of subduction or, in particular, oblique subduction processes involving old crust (Maury *et al.*, 1996; Martin *et al.*, 2005). On a global scale, there is a close relationship between low angle subducting slabs and the production of adakitic magmas (González-Partida *et al.*, 2003a), in the same way that a low angle subducting slab allows for an important modification in the thermal structure of the mantle wedge (González-Partida *et al.*, 2003a). The adakite melt forms proximal to the edges of a subduction slab at depths of 25–90 km (Thorkelson and Breitsprecher, 2005), and adakitic magmas are more likely to trigger hydrothermal convection cells more easily than other types of magmas.

In Mexico, the Laramide orogeny was the consequence of a low angle and high speed subduction processes between the Farallon and the North America plates in Late Cretaceous - early Tertiary interval (Damon *et al.*, 1981, 1983a, 1983b,). The relative changes between the Farallon and the North America plates that took place during the Late Cretaceous (Atwater, 1989), induced an inboard arc migration, caused by the shallowing of the subducting slab. The presence of adakitic rocks of ~90 Ma in east-central

Sonora, more than 200 km inland from the paleosubduction zone, has the following possible implications:

1) Although not completely understood, factors such as the trench length (>6000 km) and the plate width beneath the continent (>400 km) could have provided heterogeneous thermal conditions appropriate for the generation of magmas by partial melting.

2) Geometry of the Laramide magmatic belt during the Late Cretaceous was different from its traditionally generally accepted interpretation and, therefore, subduction was not parallel to the present northwestern coast of Mexico, but oblique.

3) Localized adakitic magmatism was not generated from melting from the Farallon oceanic plate, but from the remnants of the Mezcalera plate that was present beneath the continental crust, shortly after the Guerrero terrane accretion (Dickinson and Lawton, 2001).

The most important mineralization period in Sonora produced several porphyry copper and skarn deposits mainly during a period of ~10 m.y., between 60 and 50 Ma (Clark *et al.*, 1982; Damon *et al.*, 1983a; Staude and Barton, 2001; Barra *et al.*, 2005). This mineralization is linked to calc-alkaline magmatism. Our study shows that magmatism with an adakitic signature occurred around 90 Ma. It appears that this magmatism also generated skarn mineralization with a Cu-Zn-Ni-Co paragenesis, in the contact between the San Lucas porphyry and carbonate Paleozoic rocks, which has not been previously recognized in Sonora. Therefore, our study opens new potential opportunities for strategic mineral exploration.

ACKNOWLEDGMENTS

This work was part of Efren Pérez-Segura's doctorate research project. Pérez-Segura was supported by the University of Sonora and PROMEP grants. We are most grateful to Gilles Levresse for whole rocks analysis. This work has benefited from the critical revision of Fred McDowell and Kenneth F. Clark. The authors are grateful with Alex Pullen, William (Bill) W. Atkinson Jr., Eva Lourdes Vega-Granillo, Fernando Barra, Jaime Roldan-Quintana, Thierry Calmus and Juan Carlos García y Barragán, who helped to improve the manuscript. Analytical support for geochronology was provided by NSF EAR-0443387 (Arizona LaserChron Center).

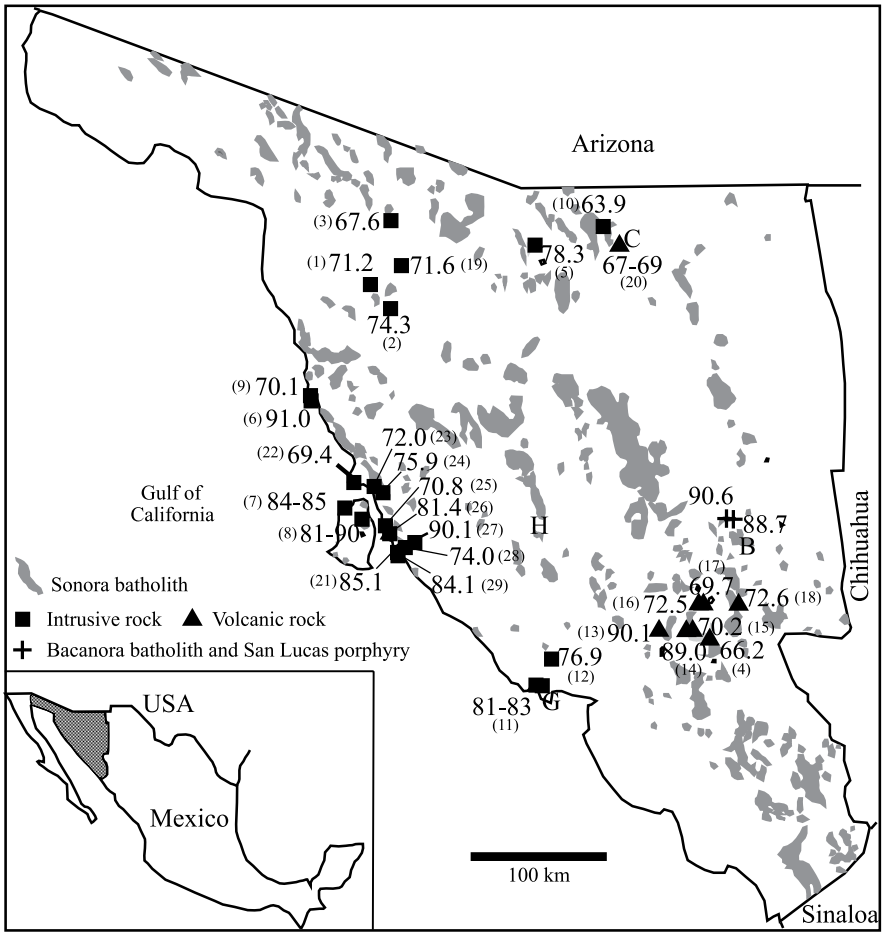

Figure 9. Selected ages older than 62 Ma for Late Cretaceous igneous rocks in Sonora, and outcrop distribution of the Sonoran batholith. C: Cananea, B: Bacanora, G: Guaymas, H: Hermosillo.

REFERENCES

Anderson, T.H., Silver, L.T., 1977, U-Pb isotope ages of granitic plutons near Cananea, Sonora: Economic Geology, 72, 827-836.

Anderson, T.H., Silver, L.T., Salas, G.A., 1980, Distribution and U-Pb isotope ages of some lineated plutons, nothwestern Mexico: Geological Society of America, Special Paper 153, 269-283.

Araux, S.E., Vega, G.R., 1984, Geología y yacimientos minerales de la Sierra La Campanería, municipio de Bacanora, Sonora Central: Hermosillo, Sonora, México, Universidad de Sonora, tesis profesional, 159 p.

Atwater, T., 1989, Plate tectonic history of the northeastern Pacific and western North America, *in* Winterer, E.L., Hussong, D.M., Decker, R.W. (eds.), The Eastern Pacific Ocean and Hawaii: Boulder, CO, Geological Society of America, The Geology of North America, v. N, 21-72.

Barra, F., Ruiz, J., Valencia, V.A., Ochoa-Landín, L., Chesley, J.T., Zurcher, L., 2005, Laramide porphyry Cu-Mo mineralization in northern México: Age constraints from Re-Os geochronology in molybdenites: Economic Geology, 100, 1605-1616.

Barton, M.D., Staude, J.M., Zürcher, L., Megaw, P.K.M., 1995, Porphyry copper and other intrusion-related mineralization in Mexico, *in* Pierce, F.W., Bolm, J.G. (eds.), Porphyry copper deposits in the American Cordillera: Arizona Geological Society Digest, 20, 487-524.

Clark, K.F., Damon, P.E., Schutter, J.R., Shafiqullah, M., 1979, Magmatismo en el norte de México en relación a los yacimientos metalíferos, *en* XIII Convención Nacional de la Asociación de Ingenieros de Minas, Metalurgistas y Geólogos de México, Acapulco, Guerrero, Memorias Técnicas, 8-57.

Clark, K.F., Foster, C.T., Damon, P.E., 1982, Cenozoic mineral deposits and subduction-related magmatic arcs in Mexico: Geological Society of America Bulletin, 93, 533-544.

Consejo de Recursos Minerales, 1996, Carta Geológico-Minera Santa Teresa H12-D45 Sonora, escala 1:50,000: Pachuca, Hidalgo, Servicio Geológico Mexicano, 1 map with abstract.

Consejo de Recursos Minerales, 2005, Carta Geológico Minera Bacanora H12-D55, Sonora, escala 1:50,000: Carta Pachuca, Hidalgo, Servicio Geológico Mexicano, 1 map with abstract.

Coney, P.J., Reynolds, S.J., 1977, Cordilleran Benioff Zones: Nature, 240, 403-406.

Damon, P.E., 1986, Batholith-volcano coupling in the metallogeny of porphyry copperdeposits, *in* Friedrich, G.H., Genkin, A.D., Naldrett**,** A.J., Ridge, J.D. (eds.), Geology and Metallogeny of Copper Deposits: Proceedings of the Copper Symposium, 27th International Geological Congress, Moscow: Berlin, Springer-Verlag, 215-234.

Damon, P.E., Shafiqullah, M., Clark, K.F., 1981, Age trends of igneous activity in relation to metallogenesis in the Southern Cordillera, *in* Dickinson, W.R., Payne, W.D. (eds.), Relations of Tectonics to Ore Deposits in Southern Cordillera: . Arizona Geological Society Digest, 14, 137-154.

Damon, P.E., Shafiqullah, M., Clark, K.F., 1983a, Geochronology of the porphyry copper deposits and related mineralization of Mexico: Canadian Journal of Earth Sciences, 20, 1052-1071.

Damon, P.E., Shafiqullah, M., Roldán-Quintana, J., Cocheme, J.J., 1983b, El batolito Laramide (90-40 Ma) de Sonora, *en* XV Convención Nacional de la Asociación de Ingenieros de Minas, Metalurgistas y Geólogos de México: Guadalajara, Jalisco, 63-95.

Defant, M.J., Drummond, M.S., 1990, Derivation of some modern arc magmas by melting of young subducted lithosphere: Nature, 347, 662-665.

Dickinson, W.R., Lawton, T.F., 2001, Carboniferous to Cretaceous assembly and fragmentation of Mexico: Geological Society of America Bulletin, 113(9), 1142-1160.

Drummond, M.S., Defant, M.J., 1990, A model for trondhjemite-tonalite-dacite genesis and crustal growth via slab melting: Archean to modern comparisons: Journal of Geophysical Research, 95(B13), 21,503-21,521.

Gans, B.P. 1997, Large magnitude Oligo-Miocene extension in southern Sonora: Implications for the tectonic evolution of northwest Mexico: Tectonics, 16, 388-408.

Gastil, R.G., Krummenacher, D., 1977, Reconnaissance geology of coastal Sonora between Puerto Lobos and Bahía Kino: Geological Society of America Bulletin, 88, 189-198.

Gehrels, G.E., Valencia, V.A., Ruiz, J., 2008, Enhanced precision, accuracy, efficiency, and spatial resolution of U-Pb ages by laser ablation multicollector inductively coupled plasma mass spectrometry: Geochemical, Geophysics. Geosystems, 9, Q03017.

González-Partida, E., Levresse, G., Carrillo-Chávez, A., Cheilletz, A., Gasquet, D., Jones, D., 2003a, Paleocene adakite Au-Fe bearing rocks, Mezcala, México: evidence from geochemical characteristics: Journal of Geochemical Exploration, 80, 25-40.

González-Partida, E., Levresse, G., Carrillo-Chávez, A., Cheilletz, A., Gasquet, D., Solorio-Munguía, J., 2003b, (Au-Fe) Skarn deposits of the Mezcala District, South-Central México: adakite association of the mineralizing fluids: International Geology Review, 45, 79-93.

González-León, C.M., McIntosh, W.C., Lozano-Santacruz, R., Valencia-Moreno, M., Amaya-Martínez, R., Rodríguez-Castañeda, J.L., 2000, Cretaceous and Tertiary sedimentary, magmatic and tectonic evolution of north-central Sonora (Arizpe and Bacanuchi Quadrangles), northwest Mexico: Geological Society of America Bulletin, 112, 600-610.

Henry, C.D., McDowell, F.W., Silver, L.T., 2003, Geology and geochronology of the granitic batholith complex, Sinaloa, México: implication for Cordilleran magmatism and tectonics, *in* Johnson, S.E., Paterson, S.R., Fletcher, J.M., Girty, G.H., Kimbrough, D.L, Martín-Barajas, A. (eds.), Tectonic Evolution of Northwestern México and the Southwestern USA: Boulder, CO, Geological Society of America, Special Paper 374, 237-273.

Hofmann, A.W., 1997, Mantle geochemistry: the message from oceanic volcanism: Nature, 385, 219-229.

Jacques-Ayala, C., García-Barragán, J.C., De Jong, K.A., Grajales, N.M., López, M., Layer, P.W., 1993, Age constraints for Cretaceous – Early Tertiary thrusting and folding in northwest Sonora, *in* González, C., Vega, L. (eds.), III Simposio de la Geología de Sonora y areas adyacentes: Hermosillo, Sonora, Universidad Nacional Autónoma de México, Instituto de Geología, Universidad de Sonora, Departamento de Geología, 61-63.

La Roche, de H., Leterrier, J., Grandclaude, P., Marchal, M., 1980, A classification of volcanic and plutonic rocks using the *R1R2* – diagram and major-element analyses its relationships with current nomenclature: Chemical Geology, 29, 183-210.

Le Maitre, R.W., Bateman, P., Dudek, A., Keller, J., Lameyre, J., Le Bas, M.J., Sabine, P.A., Schmidt, R., Sorensen, H., Streckeisen, A., Woolley, A.R., Zanettin, B, 1989, A classification of igneous rocks and glossary of terms: Recommendations of the International Union of Geological Sciences. Subcommission of the Systematics of Igneous Rocks: Oxford, Blackwell, 193 p.

Martin, H., 1987, Petrogenesis of Archaean trondhjemites, tonalites and granodiorites from Eastern Finland: major and trace element geochemistry: Journal of Petrology, 28, 921-953.

Martin H., 1999, Adakitic magmas: modern analogues of Archean granitoids: Lithos, 46, 411-429.

Martin, H., Smithies, R.H., Rapp, R., Moyen, J.F., Champion, D., 2005, An overview of adakite, tonalite-trondhjemite-granodiorite (TTG), and sanukitoid: relationships and some implications for crustal evolution: Lithos, 79, 1-24.

Maury, R.C., Sajona, F.G., Pubellier, M., Bellon, H., Defant M.J., 1996, Fusion de la croute oceanique dans les zones de subduction/collision récentes: l'exemple de Mindanao (Philippines): Bulletin de la Societé Géologique de France, 167, 579-595.

McDowell, F.W., Roldán-Quintana, J., Amaya-Martínez, R., 1997, Interrelationship of sedimentary and volcanic deposits associated with Tertiary extension in Sonora: Geological Society of America Bulletin, 109, 1349-1360.

McDowell, F.W., Roldán-Quintana, J., Connelly, J.N., 2001, Duration of late Cretaceous-early Tertiary magmatism in east-central Sonora, Mexico: Geological Society of America Bulletin, 113, 521-531.

Mead, R.D., Kesler, S.E., Foland, K.A., Jones, L.M., 1988, Relationship of Sonoran tungsten mineralization to the metallogenic evolution of Mexico, *in* Clark, K.F., Salas, G.A. (eds.), A Special Edition Devoted to the Geology and Mineral Deposits of Mexico: Economic Geology, 83, 1943-1945.

Meinert, L.D., 1982, Skarn, manto, and breccia pipe formation in sedimentary rocks of the Cananea mining district, Sonora, Mexico: Economic Geology, 77, 919-949.

Meinert, L.D., 1998, A review of skarns that contain gold, *in* Lentz, D.R. (ed.), Mineralized Intrusions-Related Skarns Systems: Mineralogical Association of Canada, Short course 26, 359-414.

Mora-Alvarez, G., McDowell, F.W., 2000, Miocene volcanism during late subduction and early rifting in the Sierra Santa Ursula of western Sonora, Mexico, *in* Delgado-Granados, H., Aguirre-Díaz, G., Stock, J.M. (eds.), Cenozoic Tectonics and Volcanism of Mexico: Geological Society of America, Special Paper 334, 123-141.

Nakamura, N., 1974, Determination of REE, Ba, Fe, Mg, Na and K in carbonaceous and ordinary chondrites: Geochimica et Cosmochimica Acta, 38, 757-775.

Ochoa-Granillo, J.A., Sosa-León, J.P., 1993, Geología y Estratigrafía de la Sierra Agua Verde con énfasis en el Paleozoico, Sonora, México: Hermosillo, Sonora, México, Universidad de Sonora, tesis profesional, 40 p.

Pérez-Segura, E., 1985, Carta metalogenética de Sonora 1:250.000, Una interpretación de la metalogenía de Sonora: Gobierno del Estado de Sonora, Dirección de Minería Geología y Energéticos, Publicación No. 7, 64 p.

Pérez-Segura, E., Gallardo-Romero, R., Valencia-Gómez, V.A., Padberg, M., 2004, La Esperanza: una nueva mineralización con Ni-Co en Sonora, México: Revista Mexicana de Ciencias Geológicas, 21(2), 260-267.

Poole, F.G., Madrid, R.J., Oliva-Becerril, F., 1991, Geological setting and origin of the stratiform barite in central Sonora, México, *in* Raines, G.L., Geology and Ore Deposits of the Great Basin: Reno, Nevada, Geological Society of Nevada, 1, 517-522.

Pubellier, M., 1987, Rélations entre le domaine Cordillerain et Mesogéen au Nord du Mexique – étude géologique de la Vallée de Sahuaripa, Sonora Central: Paris, France, Université de Paris VI, Doctorat thesis, 219 p.

Pubellier, M., Rangin, C., Rascón, B., Chorowicz, J., Bellon, H., 1995, Cenomanian thrust tectonics in the Sahuaripa region, Sonora: implications about northwestern megashears, *in* Jacques-Ayala, C., González-León, C.M., Roldán-Quintana, J. (eds.), Studies in the Mesozoic of Sonora and adjacent areas: Geological Society of America, Special Paper 301, 111-120.

Rangin, C., 1982, Contribution a l'etude géologique du systeme cordillerain du N.O. Mexique: Paris, France, Université Pierre et Marie Curie, These Doctorat d'Etat, No. 82-12.

Ramos-Velázquez, E., Calmus, T., Valencia, V., Iriondo, A., Valencia-Moreno, M., Bellon, H., 2008, U-Pb and $^{40}Ar/^{39}Ar$ geochronology of the coastal Sonora batholith: New insights on Laramide continental arc magmatism: Revista Mexicana de Ciencias Geológicas, 25(2), 314-333.

Rickwood, P.C., 1989, Boundary lines within petrologic diagrams which use oxides of major and minor elements: Lithos, 22, 247-263.

Roldán-Quintana, J., 1991, Geology and chemical composition of the Jaralito and Aconchi batholiths in east-central Sonora, México, *in* Pérez-Segura, E., Jacques-Ayala, C. (eds.), Studies in Sonoran Geology: Geological Society of America, Special Paper 254, 69-80.

Roldán-Quintana, J., 1994, Brief description of the geology and mineral deposits of southern Sonora, México, *in* Carter, L.M.H., Toth, M.I., Day, W.C. (eds.), Ninth V.E. McKelvey Forum on Mineral and Energy Resources: United States Geological Survey, Circular 1103-A, 83-84.

Roldán-Quintana, J., 2002, Caracterización geológico-geoquímica y evolución del arco magmático Mesozoico-Terciario entre San Carlos y Maycoba, sur de Sonora, México: México, D.F., Universidad Nacional Autónoma de México, tesis de doctorado, 185 p.

Schaaf, P., Roldán-Quintana, J., Calmus, T., 1999, Terrane reconnaissance in NE Sonora, México, in light of Sr-Nd-Pb isotopic data from coastal belt granitoids: Bastracts with Programs, EOS 80 (supplement), F1079-F1080.

Stacey, J.S., Kramers, J.D., 1975, Approximation of terrestrial lead isotope evolution by a two-stage model: Earth Planetary Science Letters, 26, 207–221.

Staude, J.M., Barton, M.D., 2001, Jurassic to Holocene tectonics, magmatism, and metallogeny of northwestern Mexico: Geological Society of America Bulletin, 113, 1357-1374.

Stewart, J.H., Poole, F.G., Harris, A.G., Repetski, J.E., Wardlaw, B.R., Mamet, B.L., Morales-Ramírez, J.M., 1999, Neoproterozoic(?) to Pensylvanian innershelf, miogeoclinal strata in Sierra Agua Verde, Sonora, Mexico: Revista Mexicana de Ciencias Geológicas, 16(1), 35-62.

Thorkelson, D.J., Breitsprecher, K., 2005, Partial melting of slab window margins: genesis of adakitic and non-adakitic magmas: Lithos, 79, 25-41.

Tulloch, A.J., Kimbrough, D.L., 2003, Paired plutonic belts in convergent margins and the development of high Sr/Y magmatism: Peninsular Ranges batholith of Baja-California and Median batholith of New Zealand, *in* Johnson, S.E., Paterson, S.R., Fletcher, J.M., Girty, G.H., Kimbrough, D.L., Martín-Barajas. (eds.), Tectonic Evolution of Northwestern México and the Southwestern USA: Geological Society of America, Special Paper 374, 275-295.

Valencia-Gómez, V., 2005, Evolution of La Caridad porphyry copper deposit, Sonora and geochronology of porphyry copper deposits in northwest Mexico: Tucson, Arizona, The University of Arizona, Ph. D. thesis, 197 p.

Valencia-Moreno, M., Ruiz, J., Roldán-Quintana, J., 1999, Geochemistry of Laramide granitic rocks across the southern margin of the Paleozoic North American continent, Central Sonora, Mexico: International Geology Review, 41, 1409-1422.

Valencia-Moreno, M., Ruiz, J., Barton, M.D., Patchett, P.J., Zürcher, L., Hodkinson, D.G., Roldán-Quintana, J., 2001, A chemical and isotopic study of the Laramide granitic belt of northwestern México: Identification of the southern edge of the North American Precambrian basement: Geological Society of America Bulletin, 113, 1409-1422.

Valencia-Moreno, M., Ruiz, J., Ochoa-Landín, L., Martínez-Serrano, R., Vargas- Navarro, P., 2003, Geochemistry of the Coastal Sonora batholith, Northwestern México: Canadian Journal of Earth Sciences, 40, 819-831.

Valencia, V.A., Ruiz, J., Barra, F., Gehrels, G.E., Ducea, M.N., Titley, S., Ochoa-Landín, L., 2005, U-Pb zircon and Re-Os molybdenite geochronology from La Caridad porphyry copper deposit; Insights from the duration of magmatism and mineralization in the Nacozari district, Sonora, Mexico: *Mineralium Deposita*, 40, 175-191.

Wilson, I.F., Rocha, V.S., 1946, Los yacimientos de carbón de la región de Santa Clara, mpio. de San Javier, Estado de Sonora: México, D.F., Comité Directivo para la Investigación de los Recursos Minerales de México, 9, 108 p.

Wodzicki, W.A., 1995, The evolution of the Laramide igneous rocks and porphyry copper mineralization in the Cananea District, Sonora, Mexico: Tucson, Arizona, The University of Arizona, Ph. D. thesis, 175 p.

Manuscript recieved: December 1, 2008
Corrected manuscript received: March 13, 2009
Manuscript accepted: March 15, 2009